Valence Tautomerism within a Linear Polymer Consisting of Pyrazine-Bridged Manganese−Quinone Subunits. Synthesis and Characterization of $[Mn^{III}(\mu\text{-pyz})(3,6\text{-DBSQ})(3,6\text{-DBCat})]_n$

Attia S. Attia and Cortlandt G. Pierpont*

Department of Chemistry and Biochemistry, University of Colorado, Boulder, Colorado 80309

Received June 26, 1997[⊗]

Irradiation of a hexane/THF solution of $Mn_2(CO)_{10}$, 3,6-di-*tert*-butyl-1,2-benzoquinone, and pyrazine has been used to prepare the linear [*trans*-Mn(μ-pyz)(3,6-DBQ)$_2$]$_n$ polymer. Structural characterization [monoclinic, *C*2/*m*, $Z = 2$, $a = 20.148(5)$ Å, $b = 7.547(1)$ Å, $c = 14.156(2)$ Å, $\beta = 112.23(2)°$, $V = 1992.5(6)$ Å^3, $R = 0.067$] has shown that complex subunits have an axially elongated structure that appears characteristically for d^4 Mn(III). In the solid state at room temperature, [*trans*-Mn^{III}(μ-pyz)(3,6-DBSQ)(3,6-DBCat)]$_n$ shows an electronic spectrum consisting of strong absorptions at 880 and 2090 nm, bands associated with Mn(III) redox isomers in earlier studies. Upon heating, band intensity changes in a way that indicates a reversible shift to the Mn(II) redox isomer, [*trans*-Mn^{II}(μ-pyz)(3,6-DBSQ)$_2$]$_n$. Valence tautomerism between Mn(II) and Mn(III) redox isomers is responsible for changes in equatorial Mn−O bond lengths, but with little variation in the axial Mn−N length. This is compared with the related equilibrium between Co(II) and Co(III) redox isomers of [*trans*-Co(μ-pyz)(3,6-DBQ)$_2$]$_n$ that results in large changes for both Co−O and Co−N lengths, contributing to a mechanical effect.

Introduction

Valence tautomerism has been observed to occur for a series of transition metal complexes containing semiquinonate (SQ) and catecholate (Cat) ligands chelated to Co and Mn.[1,2] Equilibria between Co^{III} and Co^{II} redox isomers (eq 1) have

$$Co^{III}(N\text{-}N)(SQ)(Cat) \rightleftharpoons Co^{II}(N\text{-}N)(SQ)_2 \qquad (1)$$

been observed by monitoring changes in electronic spectrum and magnetism that occur with the shift from low-spin Co^{III} to high-spin Co^{II}.[1] Three redox isomers are possible for the complexes of Mn, and equilibria occur in two steps (eqs 2 and 3).[2,3] Observations on equilibria are more complicated in this

$$Mn^{IV}(N\text{-}N)(Cat)^2 \rightleftharpoons Mn^{III}(N\text{-}N)(SQ)(Cat) \qquad (2)$$

$$Mn^{III}(N\text{-}N)(SQ)(Cat) \rightleftharpoons Mn^{II}(N\text{-}N)(SQ)_2 \qquad (3)$$

case. Antiferromagnetic metal−radical exchange to the SQ ligands results in an $S = {}^3/_2$ ground state for all three redox isomers, and Mn^{III} and Mn^{IV} forms of a complex have similar electronic spectra in the visible region.[2] Spectral changes in the low-energy region of the NIR have been used to observe shifts in the concentration of redox isomers shown in eq 3 in the solid state. Tautomeric equilibria have been observed for a relatively narrow collection of complexes prepared with SQ and Cat ligands derived from 3,5- and 3,6-di-*tert*-butyl-1,2-benzoquinone and with two nitrogen-donor ancillary ligands (N-N) occupying the remaining *cis* or *trans* octahedral coordination sites. Properties of equilibria have been described in terms of enthalpy and entropy changes that together define transition temperature (T_c), the point at which concentrations of redox isomers are equal.[4] Changes in metal d-orbital configuration, and specifically in the composition of the dσ antibonding orbitals directed at ligand coordination sites, result in positive values for ΔH and ΔS. Together they place T_c at a value that allows investigation of subtle ancillary ligand effects.[5] The consequent change in metal radius with dσ population results in bond length changes within the coordination sphere. Crystallographic characterization of Co^{III}(py$_2$O)(3,6-DBSQ)(3,6-DBCat) and Co^{II}(py$_2$O)(3,6-DBSQ)$_2$ has shown that the Co^{II} lengths are roughly 0.2 Å longer than similar Co^{III} values and the structural change associated with eq 1 is roughly isotropic.[1a] Microscopic changes in Co−N bond length within subunits of the pyrazine-bridged polymer [*trans*-Co(μ-pyz)(3,6-DBSQ)(3,6-DBCat)]$_n$ propagated over the length of the polymer have been used to create a macroscopic mechanical effect coupled with the change in subunit charge distribution.[6] We now describe the results of a similar study on the related polymer formed with Mn. In this case, bond length changes are anticipated to be anisotropic for the two equilibria, axial elongation for the Mn^{IV}/Mn^{III} step followed by equatorial lengthening for the second electron transfer to form Mn^{II}.

Experimental Section

Materials. 3,6-Di-*tert*-butyl-1,2-benzoquinone (3,6-DBBQ) was prepared by following a literature procedure.[7] Pyrazine and dimanganese decacarbonyl were purchased from Strem Chemical Co.

[*trans*-Mn(μ-pyz)(3,6-DBSQ)(3,6-DBCat)]$_n$. $Mn_2(CO)_{10}$ (0.17 g, 0.43 mmol), pyrazine (0.020 g, 0.25 mmol), and 3,6-DBBQ (0.33 g, 1.5 mmol) dissolved in 50 mL of 1:2 THF/hexane were combined at room temperature under N_2. The mixture was irradiated with a sunlamp

[⊗] Abstract published in *Advance ACS Abstracts,* December 15, 1997.

(1) Jung, O.-S.; Jo, D. H.; Lee, Y.-A.; Conklin, B. J.; Pierpont, C. G. *Inorg. Chem.* **1997**, *36*, 19. (b) Adams, D. M.; Dei, A.; Rheingold, A. L.; Hendrickson, D. N. *J. Am. Chem. Soc.* **1993**, *115*, 8221. (c) Abakumov, G. A.; Cherkasov, V. K.; Bubnov, M. P.; Ellert, O. G.; Dobrokhotova, Z. B.; Zakharov, L. N.; Struchkov, Yu. T. *Dokl. Akad. Nauk* **1993**, *328*, 12.
(2) Attia, A. S.; Pierpont, C. G. *Inorg. Chem.* **1995**, *34*, 1172.
(3) Attia, A. S.; Jung, O.-S.; Pierpont, C. G. *Inorg. Chim. Acta* **1994**, *226*, 91.
(4) Pierpont, C. G.; Jung, O.-S. *Inorg. Chem.* **1995**, *34*, 4281.
(5) Jung, O.-S.; Pierpont, C. G. *Inorg. Chem.* **1994**, *33*, 2227.
(6) Jung, O.-S.; Pierpont, C. G. *J. Am. Chem. Soc.* **1994**, *116*, 2229.
(7) Belostotskaya, I. S.; Komissarova, N. L.; Dzhuaryan, E. V.; Ershov, V. V. *Isv. Akad. Nauk SSSR* **1972**, 1594.

S0020-1669(97)00781-7 CCC: $14.00

Table 1. Crystallographic data for *trans*-Mn(μ-pyz)(3,6-DBSQ)(3,6-DBCat)·C_6H_{14}

empirical formula	$C_{38}H_{58}N_2O_4Mn$	V (Å^3)	1992.5(6)
fw	661.8	Z	2
space group	$C2/m$	λ(Mo Kα) (Å)	0.710 73
a (Å)	20.148(5)	D_{calcd} (g cm^{-3})	1.103
b (Å)	7.547(1)	μ (mm^{-1})	0.371
c (Å)	14.156(2)	R, R_w[a]	0.068, 0.074
β (deg)	112.23(2)		

[a] $R = \Sigma||F_o| - |F_c||/\Sigma|F_o|$. $R_w = [\Sigma w(|F_o| - |F_c|)^2/\Sigma wF_o^2]^{1/2}$.

for the period of 1 day. Slow evaporation of the solvent produced purple crystals of [*trans*-Mn(μ-pyz)(3,6-DBSQ)(3,6-DBCat)]$_n$ as a hexane solvate. Crystals were observed to form in two morphologies, thin plates that are similar to [*trans*-Co(μ-pyz)(3,6-DBSQ)(3,6-DBCat)]$_n$ and larger rhombic crystals that were subsequently used for crystallographic characterization.

IR (KBr): 2951 (vs), 2909 (sh), 2865 (sh), 1558 (s), 1481 (vs), 1464 (m), 1452 (sh), 1429 (m), 1416 (vs), 1378 (vs), 1356 (m), 1319 (w), 1283 (s), 1220 (w), 1169 (vs), 1157 (sh), 1127 (w), 1036 (m), 976 (s), 948 (w), 939 (sh), 927 (w) cm^{-1}.

Physical Measurements. Electronic spectra were recorded on a Perkin-Elmer Lambda 9 spectrophotometer. Magnetic measurements were made using a Quantum Design SQUID magnetometer at a field of 5 kG. Infrared spectra were recorded on a Perkin-Elmer 1600 FTIR instrument with samples prepared as KBr pellets.

Crystallographic Characterization of [*trans*-Mn(μ-pyz)(3,6-DBSQ)(3,6-DBCat)]$_n$. A dark purple rhombic crystal was mounted, coated with an amorphous resin, and aligned on a Siemens P3F automated diffractometer. The centered settings of 25 reflections in the 2Θ range 21.0−36.0° were used to obtain the unit cell dimensions listed in Table 1. An independent quadrant of data was collected. Crystals were found to form in the monoclinic crystal system, space group $C2/m$, with $Z = 2$. A difference Fourier map calculated with the Mn atom located at the origin of the unit cell revealed the positions of other independent non-hydrogen atoms of the complex. A subsequent difference Fourier map gave the locations of independent carbon atoms associated with the hexane molecule of crystallization.

Results and Discussion

Synthesis and Structure of Polymeric [*trans*-Mn(μ-pyz)(3,6-DBSQ)(3,6-DBCat)]$_n$. The addition of *o*-benzoquinones to metal carbonyl complexes has been used to provide semiquinone and catecholate complexes by transfer of charge from the neutral metal to the quinone ligands. Metal oxidation and quinone ligand reduction are influenced by the donation effects of other ancillary ligands in the reaction medium. With 4-nitro-1,10-phenanthroline, the Mn(II) redox isomer $Mn^{II}(NO_2\text{-phen})(3,6\text{-DBSQ})_2$ has been formed in reactions that begin with $Mn_2(CO)_{10}$ and 3,6-DBBQ.[2] Similar procedures carried out with either 4,4'-bipyridine or pyridine as coligands lead to the formation of *trans* redox isomers of different charge distributions. With 4,4′-bipyridine, *trans*-$Mn^{III}(4,4'\text{-bpy})_2$(3,6-DBSQ)(3,6-DBCat) was obtained, while with pyridine and 4-*tert*-butylpyridine, the Mn(IV) redox isomer *trans*-$Mn^{IV}(py)_2$(3,6-DBCat)$_2$ was formed.[2,3] Spectroscopic evidence for tautomeric equilibria was recorded for both compounds in solution and in the solid state. In the presence of pyrazine, photolysis of a $Mn_2(CO)_{10}$/3,6-DBBQ mixture in hexane gives crystals of polymeric [Mn(μ-pyz)(3,6-DBQ)$_2$]$_n$ as the hexane solvate. Crystals were observed to form in two morphologies, thin plates and rhombic parallelepipeds, depending on the crystallization medium. Plates obtained from pure hexane were found to form in the same tetragonal unit cell as [Co(μ-pyz)(3,6-DBSQ)(3,6-DBCat)]$_n$. Crystallization from a THF/hexane mixture gave large monoclinic parallelepipeds, and a crystal from this sample was used for crystallographic characterization. Hemispheres of redundant reflections were measured to confirm differences in Laue symmetry for the unit cells, and reflections were scanned to verify that crystals were not twinned. The tetragonal unit cell of [Co(μ-pyz)(3,6-DBSQ)(3,6-DBCat)]$_n$ had complex subunits located at positions of general symmetry, and SQ and Cat ligands were distinguishable on the basis of characteristic differences in bond lengths. Site symmetry of the Mn atom of [Mn(μ-pyz)(3,6-DBQ)$_2$]$_n$ in the monoclinic unit cell imposes $2/m$ symmetry on the complex subunit. Quinone ring carbon and oxygen atoms lie on the mirror plane, and the 2-fold axis bisects the pyrazine ligand. Upper and lower portions of the pyrazine ring are related by translational symmetry. A view of one subunit is shown in Figure 1. The hexane molecule of crystallization is also located about a site of crystallographic $2/m$ symmetry. A view showing a plane of polymer strands with hexane solvate molecules located at voids between strands is shown in Figure 2. The tetragonal unit cell consists of stacks of planes alternately rotated by 90°, while the packing arrangement in the monoclinic cell consists of stacked planes of parallel strands.

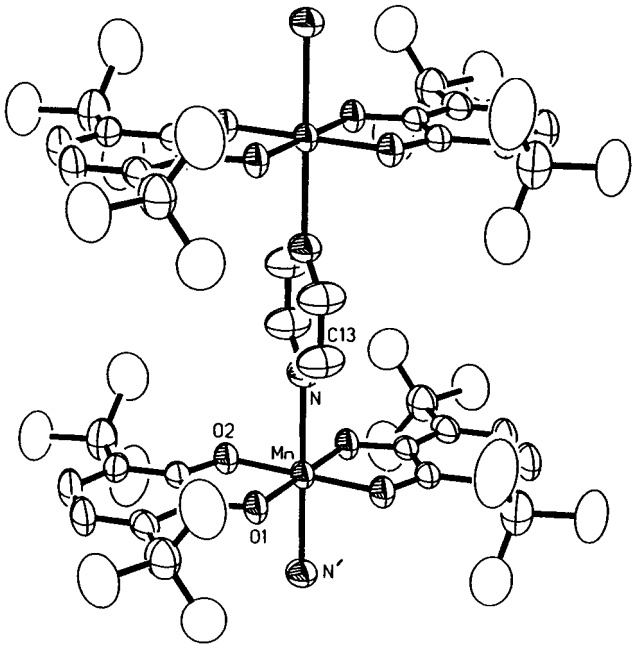

Figure 1. View showng one subunit of the Mn^{III}(μ-pyz)(3,6-DBSQ)(3,6-DBCat) polymer.

Symmetry imposed on the complex subunit in the monoclinic unit cell relates the two quinone ligands, perhaps pointing to a Mn(IV) charge distribution that is similar to that in *trans*-$Mn^{IV}(py)_2$(3,5-DBCat)$_2$.[8] Bond lengths within the inner coordination sphere are more similar to those of *trans*-$Mn^{III}(4,4'\text{-bpy})_2$(3,6-DBSQ)(3,6-DBCat), however.[2] Bond lengths are listed in Table 2 with lengths of related manganese−quinone complexes. The axial Mn−N length is 2.375(5) Å, slightly longer than the 2.273(7) Å value of *trans*-$Mn^{III}(4,4'\text{-bpy})_2$(3,6-DBSQ)(3,6-DBCat) and considerably longer than values of 2.018(3) and 2.034(11) Å for the Mn(IV) complexes *trans*-$Mn^{IV}(py)_2$(3,5-DBCat)$_2$ and *trans*-Mn^{IV}(Bupy)$_2$(3,6-DBCat)$_2$.[2,3] Equatorial Mn−O lengths of 1.878(3) and 1.885(3) Å compare well with the average Mn−O length of 1.886(4) Å for the Mn(III) 4,4'-bpy complex and are slightly longer than the Mn(IV) values of 1.854(2) and 1.861(10) Å (Table 2). The axially elongated structure of [Mn(μ-pyz)(3,6-DBQ)$_2$]$_n$ is a clear signature of Mn(III). With the Mn(III) charge distribution for [Mn^{III}(μ-pyz)(3,6-DBSQ)(3,6-DBCat)]$_n$, structural features of the mixed-charge quinone

(8) Lynch, M. W.; Hendrickson, D. N.; Fitzgerald, B. J.; Pierpont, C. G. *J. Am. Chem. Soc.* **1984**, *106*, 2041.

Table 2. Inner Coordination Sphere Bond Lengths (Å) for Manganese−Quinone Redox Isomers

compound	Mn−O	Mn−N	C−O_{av}	ref
$Mn^{III}(\mu$-pyz)(3,6-DBSQ)(3,6-DBCat)	1.878(3), 1.885(3)	2.375(5)	1.330(9)	
$Mn^{IV}(py)_2$(3,5-DBCat)$_2$	1.853(2), 1.854(2)	2.018(3)	1.348(4)	8
$Mn^{IV}(Bupy)_2$(3,6-DBCat)$_2$	1.854(10), 1.868(10)	2.034(11)	1.347(19)	3
Mn^{III}(4,4′-bpy)$_2$(3,6-DBSQ)(3,6-DBCat)	1.883(4), 1.889(5)	2.273(7)	1.335(8)	2
$Mn^{II}(NO_2phen)$(3,6-DBSQ)$_2$	2.133(5)−2.148(5)	2.283(7), 2.296(6)	1.268(9)	2

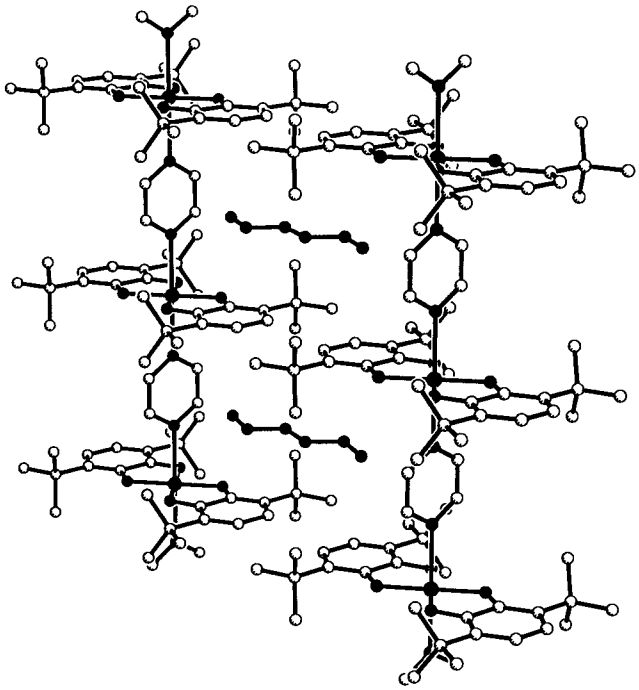

Figure 2. View of the polymer strands and the hexane solvate molecule for $Mn^{III}(\mu$-pyz)(3,6-DBSQ)(3,6-DBCat)·C_6H_{14}.

ligands are either disordered or averaged by interligand charge transfer. Features of the symmetrically unique ligand are very similar to those of the independent quinone ligand of Mn^{III}-(4,4′-bpy)$_2$(3,6-DBSQ)(3,6-DBCat), where crystallographic inversion symmetry is imposed on the molecule.

Spectral and Magnetic Properties of [$Mn^{III}(\mu$-pyz)(3,6-DBSQ)(3,6-DBCat)]$_n$. Electronic spectra recorded for a solid sample of [$Mn^{III}(\mu$-pyz)(3,6-DBSQ)(3,6-DBCat)]$_n$ further confirm the Mn(III) charge for the metal. An interligand charge transfer transition appears characteristically for Mn^{III}(SQ)(Cat) species in the 2100 nm region of the NIR,[2] and an intense transition appears at 2090 nm for the pyrazine polymer at room temperature. Temperature-dependent changes in the intensity of this transition provide a way of monitoring shifts in equilibria between redox isomers. The appearance of a transition in this region for $Mn^{IV}(Bupy)_2$(3,6-DBCat)$_2$ at 350 K indicated a shift to $Mn^{III}(Bupy)_2$(3,6-DBSQ)(3,6-DBCat). When the temperature of the [$Mn^{III}(\mu$-pyz)(3,6-DBSQ)(3,6-DBCat)]$_n$ sample was increased from room temperature, a *decrease* in the intensity of the 2090 nm transition was observed and the band shifted to lower energy (Figure 3). Entropy changes are positive for the equilibrium shifts shown in eqs 2 and 3 due to low-frequency shifts in vibrational modes and increased conformational flexibility with the change in metal d configuration from d^3 to hs-d^5. Shifts that occur for these equilibria with increasing temperature favor the higher d configuration. Consequently, the decrease in band intensity at 2090 nm with increasing temperature reflects a shift from Mn(III) to Mn(II) (eq 4). A

$$[Mn^{III}(\mu\text{-pyz})(3,6\text{-DBSQ})(3,6\text{-DBCat})]_n \rightarrow [Mn^{II}(\mu\text{-pyz})(3,6\text{-DBSQ})_2]_n \quad (4)$$

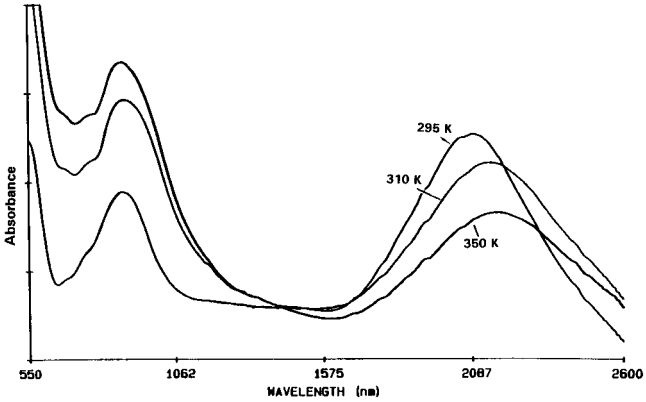

Figure 3. Electronic spectra recorded on a solid (KBr) sample of Mn^{III}-(μ-pyz)(3,6-DBSQ)(3,6-DBCat) showing temperature-dependent changes in band intensity with the shift to $Mn^{II}(\mu$-pyz)(3,6-DBSQ)$_2$.

transition at 880 nm appears for both the Mn(III) and Mn(IV) redox isomers,[2,3] and a strong band appears at this position for [$Mn^{III}(\mu$-pyz)(3,6-DBSQ)(3,6-DBCat)]$_n$. The intensity of this band decreases with increasing temperature in accord with the shift to the Mn(II) redox isomer, but the development of an intense transition further toward the UV region results in a general increase in background across this region of the visible spectrum in the solid state. Toluene solutions of [$Mn^{III}(\mu$-pyz)-(3,6-DBSQ)(3,6-DBCat)]$_n$ at room temperature are pale brown-green due to weak transitions in the 420 and 750 nm regions. Bands appear at these positions for [Mn^{II}(3,5-DBSQ)$_2$]$_4$, for $Mn^{II}(py)_2$(3,5-DBSQ)$_2$, and generally for the Mn(II) redox isomers Mn^{II}(N-N)(DBSQ)$_2$ that form for most members of the series in nonpolar solvents at room temperature.[2] Upon cooling, solutions turn to the intense purple color of the Mn(III) and Mn(IV) isomers.

Magnetic measurements on the redox isomers of Mn provide little information on equilibrium shifts, in contrast to the related complexes of Co, where the transition from ls-Co(III) to hs-Co(II) results in a dramatic increase in magnetic moment. Antiferromagnetic coupling between dπ spins of the metal ion and the radical SQ ligands results in an $S = {}^3/_2$ ground state for both the Mn^{II} and Mn^{III} redox isomers. The temperature dependence of magnetic moment is the result of shifts in equilibria, the thermal population of higher order spin states for isomers of both charge distributions, and orbital effects. The magnetic behavior of [$Mn^{III}(\mu$-pyz)(3,6-DBSQ)(3,6-DBCat)]$_n$ follows the general pattern observed for other related Mn−quinone complexes in showing a gradual drop from 4.3 μ_B at 350 K to 3.8 μ_B at 30 K and a sharper decrease to 3.4 μ_B at 5 K. A plot of magnetic moment *vs* temperature is shown in Figure 4. The similarity to related monomeric complexes of Mn indicates that exchange between metals through the pyrazine bridge is insignificant.[2,3]

Valence Tautomerism and Associated Single-Crystal Mechanical Properties. Changes in the length of individual bonds aligned along the linear axis of a one-dimensional polymer may produce a macroscopic change in polymer length. Metal−quinone electron transfer, induced either optically or thermally, results in a change in the electronic structure of the metal ion and, in select cases, in metal radius and ligand bond lengths.

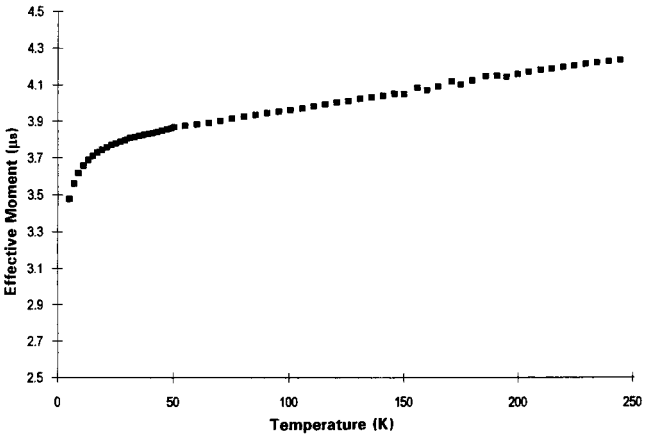

Figure 4. Changes in magnetic moment for $Mn^{III}(\mu$-pyz)(3,6-DBSQ)(3,6-DBCat) over the temperature range 5−250 K. Magnetic moment continues to increase to 4.3 μ_B at 350 K.

This has been described in detail for the Co^{III}(Cat)/Co^{II}(SQ) couple.[6] Excitation, and the associated change in polymer length, may be carried out anisotropically by irradiating a crystal of the highly colored polymer from a direction perpendicular to the linear axis. Length change occurs on the irradiated side of the crystal, polymer subunits on the dark side remain in the ground state, and the anisotropic change in axial length results in a mechanical response to irradiation. The photomechanical effect has been described for $Rh(CO)_2$(3,6-DBSQ),[9] and measurements on crystal bend angle versus energy of incident light map the transition at 1550 nm that is responsible for the crystal-bending effect in this case. Photomechanical effects have also been reported for complexes of Co. Crystals of Co(bpy)(3,6-DBSQ)(3,6-DBCat) respond to light excitation, although studies on energy dependence have not yet been carried out.[1c] In the solid state lattice of Co(bpy)(3,6-DBSQ)(3,6-DBCat), molecules stack in columns with bipyridine ligands atop one another.[1c,5] We have been investigating supported polymers in an effort to form more robust materials that show photomechanical properties. The compound of initial interest was the pyrazine-bridged linear polymer [*trans*-Co(μ-pyz)(3,6-DBSQ)(3,6-DBCat)]$_n$.[6] Tetragonal crystals of the material form as thin plates that were observed to curl reversibly upon irradiation with light from a tungsten lamp. Crystals form as an unstable hexane solvate requiring that experiments be conducted at low temperature, and difficulties in obtaining sufficient data on thin crystals of low volume resulted in a relatively imprecise crystal structure of the polymer. Observations on tautomeric equilibria for Mn−quinone complexes, with associated changes in bond length, make the [Mn(μ-pyz)(3,6-DBQ)$_2$]$_n$ polymer of interest as a compound that may exhibit bimodal mechanical properties. Mn^{IV}/Mn^{III} and Mn^{III}/Mn^{II} steps described in eqs 2 and 3 result in an initial change in axial length (eq 2), followed by the change in equatorial Mn−O lengths for the *trans* isomer shown below.

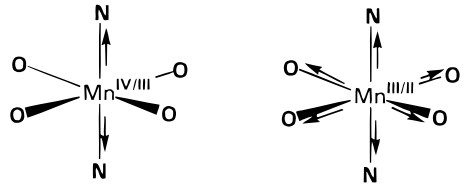

Structural and spectroscopic characterization of [Mn(μ-pyz)(3,6-DBQ)$_2$]$_n$ shows that it exists in the solid state at room temperature in the form of the Mn(III) redox isomer and the shift in charge distribution that occurs at increased temperature is to the Mn(II) isomer. Bond length changes occur normal to the polymer length, and consequently, crystals of [Mn(μ-pyz)(3,6-DBSQ)(3,6-DBCat)]$_n$ fail to exhibit mechanical properties.

It seems possible to form extended polymers consisting of metal−quinone subunits with relative ease by using adaptations of the synthetic procedures that have been developed to give molecular complexes. The soft lattice formed using ligands that have *tert*-butyl substituents permits structural distortions in the solid state that accompany changes in metal charge and spin state without disruption of the crystal structure.

Acknowledgment. We thank Dr. Brenda Conklin for recording magnetic measurements, the NIST Laboratory in Boulder, CO, for allowing access to its SQUID magnetometer, and Professor M. F. El-Shahat of Ain Shams University for helpful comments. Support for this research was provided by the National Science Foundation and by the Egyptian Ministry of Science (A.S.A.) through a graduate fellowship.

Supporting Information Available: Complete listings of crystallographic details, atomic coordinates, bond lengths and bond angles, thermal displacement parameters, and calculated hydrogen positional parameters for *trans*-Mn(μ-pyz)(3,6-DBSQ)(3,6-DBCat)·C_6H_{14} (9 pages). Ordering information is given on any current masthead page.

IC970781D

(9) Lange, C. W.; Foldeaki, M.; Nevodchikov, V. I.; Cherkasov, V. K.; Abakumov, G. A.; Pierpont, C. G. *J. Am. Chem. Soc.* **1992**, *114*, 4220.